The GALAH Survey: Chemically tagging the Fimbulthul stream to the globular cluster ω Centauri

Jeffrey D. Simpson [1]*, Sarah L. Martell [1,2], Gary Da Costa [3], Jonathan Horner,[4]
Rosemary F. G. Wyse,[5] Yuan-Sen Ting,[6,7,8] Martin Asplund,[2,3]
Joss Bland-Hawthorn [2,9], Sven Buder [10], Gayandhi M. De Silva,[2,11]
Ken C. Freeman,[3] Janez Kos,[9,12] Geraint F. Lewis [9], Karin Lind,[10,13]
Sanjib Sharma [2,9], Daniel B. Zucker,[2,14] Tomaž Zwitter [12], Klemen Čotar [12],
Peter L. Cottrell[15,16] and Thomas Nordlander [2,3]

[1]*School of Physics, UNSW, Sydney, NSW 2052, Australia*
[2]*Centre of Excellence for Astrophysics in Three Dimensions (ASTRO-3D), Australia*
[3]*Research School of Astronomy & Astrophysics, Australian National University, ACT 2611, Australia*
[4]*Centre for Astrophysics, University of Southern Queensland, Toowoomba, QLD 4350, Australia*
[5]*Department of Physics and Astronomy, Johns Hopkins University, Baltimore, MD 21218, USA*
[6]*Institute for Advanced Study, Princeton, NJ 08540, USA*
[7]*Department of Astrophysical Sciences, Princeton University, Princeton, NJ 08544, USA*
[8]*Observatories of the Carnegie Institution of Washington, 813 Santa Barbara Street, Pasadena, CA 91101, USA*
[9]*Sydney Institute for Astronomy, School of Physics, A28, The University of Sydney, NSW 2006, Australia*
[10]*Max Planck Institute for Astronomy (MPIA), Koenigstuhl 17, D-117 Heidelberg, Germany*
[11]*Australian Astronomical Optics, Faculty of Science and Engineering, Macquarie University, Macquarie Park, NSW 2113, Australia*
[12]*Faculty of Mathematics and Physics, University of Ljubljana, Jadranska 19, 1000 Ljubljana, Slovenia*
[13]*Department of Physics and Astronomy, Uppsala University, Box 517, SE-751 20 Uppsala, Sweden*
[14]*Department of Physics and Astronomy, Macquarie University, Sydney, NSW 2109, Australia*
[15]*School of Physical and Chemical Sciences, University of Canterbury, Christchurch, New Zealand*
[16]*Monash Centre for Astrophysics, School of Physics and Astronomy, Monash University, Melbourne, Australia*

ABSTRACT

Using kinematics from *Gaia* and the large elemental abundance space of the second data release of the GALAH survey, we identify two new members of the Fimbulthul stellar stream, and chemically tag them to massive, multimetallic globular cluster ω Centauri. Recent analysis of the second data release of *Gaia* had revealed the Fimbulthul stellar stream in the halo of the Milky Way. It had been proposed that the stream is associated with the ω Cen, but this proposition relied exclusively upon the kinematics and metallicities of the stars to make the association. In this work, we find our two new members of the stream to be metal-poor stars that are enhanced in sodium and aluminium, typical of second population globular cluster stars, but not otherwise seen in field stars. Furthermore, the stars share the s-process abundance pattern seen in ω Cen, which is rare in field stars. Apart from one star within 1.5 deg of ω Cen, we find no other stars observed by GALAH spatially near ω Cen or the Fimbulthul stream that could be kinematically and chemically linked to the cluster. Chemically tagging stars in the Fimbulthul stream to ω Cen confirms the earlier work, and further links this tidal feature in the Milky Way halo to ω Cen.

Key words: globular clusters: individual: ω Cen – galaxy: halo – galaxy: kinematics and dynamics.

1 INTRODUCTION

The modern paradigm for the formation and growth of galaxies, and of larger scale structures within the Universe (known as the ΛCDM paradigm) features the growth of large galaxies, like the Milky Way,

* E-mail: jeffrey.simpson@unsw.edu.au

through mergers with smaller bodies (e.g. Searle & Zinn 1978; White & Frenk 1991; Côté, Marzke & West 1998; Côté et al. 2000; Cole et al. 2002; Venn et al. 2004; Oser et al. 2010). When a dwarf galaxy merges with Milky Way, it is tidally stripped of some, or all, of its stars. Similarly, objects already orbiting the Milky Way can be tidally stripped of stars during events like Galactic plane passages. If the dynamical evolution time-scale is larger than the orbital period, these stripped stars remain for some time on approximately the mean orbit of the progenitor (Lynden-Bell & Lynden-Bell 1995). This leads to streams and tidal debris throughout the Milky Way Galaxy, acting as the fossils records of these events.

Large-scale photometric surveys have, to date, uncovered some 50 streams in our Galaxy (Mateu, Read & Kawata 2018, and references therein). The second data release of the ESA's *Gaia* mission (Prusti et al. 2016; Brown et al. 2018) has caused an explosion in the discovery rate of streams through the combination of precise photometry and proper motion measurements, and has been used to identify stellar streams in the local region of the Galaxy (Meingast, Alves & Fürnkranz 2019), the bulge (e.g. Ibata et al. 2018), the halo (e.g. Koppelman, Helmi & Veljanoski 2018; Malhan, Ibata & Martin 2018; Ibata, Malhan & Martin 2019b), and even potentially outside of our Galaxy in the Magellanic Stream (e.g. Price-Whelan 1; Price-Whelan et al. 2018a; Bellazzini et al. 2019; Nidever et al. 2019). There is much interest in kinematically mapping these streams (e.g. Li et al. 2019) as they are a useful tool for studying our Galaxy's history and large-scale structure (Eyre & Binney 2009; Law & Majewski 2010; Bonaca et al. 2019; Malhan & Ibata 2019).

A number of extant star clusters have been found to have extratidal features or streams associated with them (e.g. Odenkirchen et al. 2001; Belokurov et al. 2006; Olszewski et al. 2009; Kuzma, Da Costa & Mackey 2018; Carballo-Bello 2019; Palau & Miralda-Escudé 2019). Such links are particularly valuable, as they can provide a strong test for models of the gravitational field of the Milky Way. Simply put, any successful model must correctly predict the location and motion of the stream relative to the progenitor cluster.

Ibata et al. (2019b) identified a new cluster-stream pairing using *Gaia* DR2, finding that the massive globular cluster ω Cen could be linked to one of their newly discovered streams, which they named Fimbulthul. They found that Fimbulthul and ω Cen had similar orbital energies and angular momenta. The relationship was explored further in Ibata et al. (2019a, hereafter I + 19), where the authors estimated the metallicities of four stream members, finding them to be metal poor. Since I + 19 had only metallicities for their stars to compare to ω Cen, and ω Cen has a large metallicity range ($-2.0 <$ [Fe/H] < -0.5; e.g. Johnson & Pilachowski 2010), it is prudent to explore a larger set of elemental abundance distributions of the stream stars, and to determine if they can be chemically tagged to ω Cen. The chemical tagging of stars in streams to progenitors is a burgeoning field of research. Hasselquist et al. (2019) found ∼30 stars in the APOGEE survey that had kinematics consistent with those predicted by N-body simulations of the Sagittarius dwarf spheroidal galaxy stream and chemical abundances like those found in it.

In general, chemically tagging stars to globular clusters takes advantage of the fact that almost[1] every Milky Way globular cluster studied in detail exhibits star-to-star variations in light-element abundances,[2] typically with anticorrelations between [O/Fe] & [Na/Fe], and [Mg/Fe] & [Al/Fe]. In globular cluster research, the stars with abundance patterns like the Galactic halo (e.g. low sodium and high oxygen) are commonly referred to as 'primordial' or 'first population' stars. The stars with enhanced abundances of sodium and depleted oxygen are 'enriched' or 'second population' stars. It is these second population stars that can be most readily identified in the field (as they are only about ∼2 per cent of the halo, e.g. Martell et al. 2011) and chemically tagged as having come from globular clusters (e.g. Martell & Grebel 2010; Fernández-Trincado et al. 2016, 2017; Schiavon et al. 2017; Tang et al. 2019).

In addition to the light element abundance dispersions, ω Cen exhibits large metallicity and s-process element abundance ranges (e.g. Norris & Da Costa 1995b; Johnson & Pilachowski 2010; Marino et al. 2012; Simpson, Cottrell & Worley 2012; Simpson & Cottrell 2013), neither of which are typically observed in globular clusters (there are some notable exceptions, e.g. M22; Marino et al. 2011a). Along with its retrograde orbit about the Milky Way, these abundance patterns have led to the hypothesis that ω Cen is the core of an accreted dwarf galaxy (Bekki & Freeman 2003). If so, there should be a large amount of tidal debris in the Milky Way halo that was stripped from ω Cen's parent galaxy.

There have been many searches for such stars. The obvious place to search for tails is within 10 deg of the cluster, where the kinematic and distance properties will still be similar to those of the cluster. Marconi et al. (2014) and I + 19 both find evidence for tails in star counts. While those photometric surveys have provided some evidence for extratidal features, spectroscopic searches within a few degrees have not identified significant quantities of ω Cen stars beyond the tidal radius. Da Costa & Coleman (2008) searched up to 2 deg from the cluster and found only six stars outside the tidal radius with radial velocities expected for ω Cen – and we note that with *Gaia* proper motions only two of these are consistent with membership.

A few field stars have been associated with ω Cen. Lind et al. (2015) found a star with low [Mg/Fe] and high [Al/Fe] that they conjectured could have been ejected at high speed from ω Cen. Fernández-Trincado et al. (2015) found eight stars in RAVE that they calculated to have been ejected from ω Cen. Both of these works warrant follow-up in light of the new precision proper motions from *Gaia*. Myeong et al. (2018) identified retrograde substructures in the halo based upon clustering in action space, and some of these structures they associated with ω Cen.

In this work we aim to chemically tag stars of the Fimbulthul stream to ω Cen using the second data release of the GALactic Archaeology with HERMES (GALAH) survey (De Silva et al. 2015; Buder et al. 2018). The GALAH survey is a large and ambitious spectroscopic investigation of the local stellar environment. One of its principal aims is to determine precise abundances of up to 30 elements from one million stars, and to use chemical tagging to identify dispersed stellar clusters in the field of the disc and halo (for the initial motivating chemical tagging papers, see Freeman & Bland-Hawthorn 2002; Bland-Hawthorn, Krumholz & Freeman 2010). The results from the GALAH survey have already been used to explore stellar streams (Quillen et al. 2018), have shown that chemical tagging can work on comoving pairs of stars (Simpson et al. 2019), and have found additional members of the Pleiades (Kos et al. 2017). It has also had the interesting

---

[1]The notable exception is Ruprecht 106 (Villanova et al. 2013; Dotter et al. 2018).

[2]The formation mechanisms of globular clusters are hotly debated; see the review of Bastian & Lardo (2018) and references therein.

null result of showing that several purported clusters do not exist (Kos et al. 2018).

This paper is structured as follows: we describe the data sets used in Section 2, the spatial and kinematic identification of stream stars in Section 3, the chemical tagging of the stars to ω Cen in Section 4, and we present our conclusions in Section 5.

2 DATA

In this work, we use the second public data release of the GALAH survey (GALAH DR2; see the release paper: Buder et al. 2018), as well as ω Cen stars observed by GALAH that were not part of the public release. Overall, this gives 375 688 stars with up to 23 elemental abundances per star. The GALAH survey's observing procedures can be found in Martell et al. (2017). In-depth descriptions of the spectral reduction, stellar parameter, and abundance inference pipelines can be found in Kos et al. (2016) and Buder et al. (2018). Below we will briefly describe the details from those papers pertinent to this work.

These data are based upon spectra obtained between 2013 November and 2017 September using the 3.9-m Anglo-Australian Telescope with the HERMES spectrograph (Sheinis et al. 2015) and the Two-Degree Field fibre positioner top-end (Lewis et al. 2002). HERMES simultaneously acquires spectra for $\sim$360 science targets using four independent cameras with non-contiguous wavelength coverage totalling $\sim$1000 Å at a spectral resolving power of $R \approx 28\,000$. The spectra were reduced using an IRAF-based pipeline that was developed specifically for GALAH and optimized for speed, accuracy, and consistency (Kos et al. 2016).

The GALAH DR2 stellar parameter and abundance pipeline used a two-step process (Buder et al. 2018). In the first step, spectra with high signal-to-noise were identified and analysed with the spectrum synthesis code Spectroscopy Made Easy (SME; Valenti & Piskunov 1996; Piskunov & Valenti 2016) to determine the stellar labels (e.g. $T_{\rm eff}$, log g, [Fe/H], $v_{\rm mic}$, $v\sin i$, $v_{\rm rad}$, and [X/Fe]). In the second step, THE CANNON (Ness et al. 2015) learned these training set labels from SME and built a quadratic model at each pixel of the normalized spectrum as a function of the labels. Abundance estimates were then generated from THE CANNON model for all of the spectra. It is these THE CANNON values that we use in this work.

For some stars, the label results from THE CANNON are not necessarily reliable. For stellar parameters, these are flagged in the `flag_cannon` value, and for individual elements in the `flag_x_fe` value (where x is the element symbol). Buder et al. (2018) recommends to only use stellar parameters from stars where `flag_cannon = 0`, and for a given elemental abundance where `flag_x_fe = 0`. However, this would restrict the number of possible ω Cen-like stars we could investigate, as the training set was not highly populated at the metal-poor end of the iron abundance distribution function. Of the 9090 stars in the data set with [Fe/H] < -1.0, only 66 per cent (5987/9090) have `flag_cannon = 0`, and 1929 stars have `flag_cannon = 1` (this indicates that THE CANNON started to extrapolate outside of the training set bounds to estimate the abundance). For the elements of interest for chemical tagging stars to ω Cen, many of the metal-poor stars would be excluded with a strict flagging criterion: for [Na/Fe] and [Ba/Fe] only $\sim$2700 stars of these metal-poor stars have `flag_x_fe = 0`, and for [Al/Fe] it is only 628 stars. In this work, we decided to loosen the flagging criteria and use iron abundance values for stars where `flag_cannon` $\in \{0, 1\}$ (i.e. no flags; or THE CANNON started to extrapolate) and individual elemental abundances where `flag_x_fe` $\in \{0, 1, 2\}$ (i.e. no flags; THE CANNON started to extrapolate; or line strength was below the 2-σ upper limit). This increases the number of useful stars to 7916, 4326, 5225, and 1886 for [Fe/H], [Na/Fe], [Ba/Fe], and [Al/Fe] respectively.

The GALAH survey data were combined with the astrometric and proper motion data from the second data release (DR2) from the *Gaia* mission. GALAH's input catalogue is based upon 2MASS (Skrutskie et al. 2006), so we used the `tmass_best_neighbour` table produced by the *Gaia* collaboration for the cross-match. To exclude stars with likely poor astrometry, we required that the Renormalized Unit Weight Error (defined in Lindegren 2018) be <1.4. As *Gaia* photometry is less reliable in crowded regions (e.g. globular clusters) due to source confusion in the blue and red photometers (Evans et al. 2018), we excluded stars which did not fall in the range $1.0 + 0.015(G_{\rm BP} - G_{\rm RP})^2 < CE < 1.3 + 0.06(G_{\rm BP} - G_{\rm RP})^2$, where CE is the `phot_bp_rp_excess_factor` (Babusiaux et al. 2018).

From both the GALAH data set and the full *Gaia* data set we identified likely ω Cen members. For both data sets we selected stars within 1 deg of (RA, Dec) = (201.697°, −47.480°), proper motions within 2 mas yr^{-1} of ($\mu_{\rm RA}$, $\mu_{\rm Dec}$) = (− 3.1925, −6.7445) mas yr^{-1} (Helmi et al. 2018), and parallaxes of $|\varpi| < 1$ mas. The proper motion distance of <2 mas yr^{-1} was selected as it encompassed an obvious overdensity in the proper motion distribution of the GALAH-observed stars. The systemic radial velocity of ω Cen has a large offset from the bulk of stars along the line-of-sight: 232 km s^{-1} (see e.g. Da Costa & Coleman 2008). For the GALAH data set we required that every star be within 40 km s^{-1} of this value. For the *Gaia* data set, the bulk of stars do not have measured radial velocities, so we excluded only the few stars that met the other criteria but were outside the 232 ± 40 km s^{-1} range. In total, these selection criteria identified 352 members of ω Cen observed by the GALAH survey (with a radial velocity mean and standard deviation of 232.9 ± 8.6 km s^{-1}), and 66 597 from *Gaia* DR2.

3 IDENTIFICATION OF NEW CANDIDATE STREAM MEMBERS

The proposed Fimbulthul stream members (from supplementary table 1 of I + 19) are dominated by dwarf stars with a handful of giant stars. With a distance of $\sim$4 kpc, almost all of the stream stars are much fainter than the typical apparent magnitude range observed by GALAH ($12 < V < 14$), and none of the proposed stream members were observed by GALAH.

The STREAMFINDER software (Malhan & Ibata 2018) as implemented by Ibata et al. (2019b) avoided the region within 30 deg of the Galactic plane due to confusion from the high stellar density and differential reddening. This means that they excluded stars within $\sim$15 deg of ω Cen, so we extended our search for possible Fimbulthul stars into this 'zone of avoidance'. We also looked along the known stream region for stars observed by GALAH to identify if there were stars that also shared the kinematics of the known stream stars that may have been missed by Ibata et al. (2019b).

Fig. 1 shows the stars observed by GALAH in the region of the sky around ω Cen and the Fimbulthul stream, as well as the Fimbulthul members identified by I + 19. Along the known stream region (i.e. $b > 30$ deg), we selected stars observed by GALAH that were from fields with centres within 4 deg of the fiducial line of the stream and applied the following selection criteria: radial velocity in the range $150 < v_{\rm rad} < 300$ km s^{-1} (the radial velocities predicted
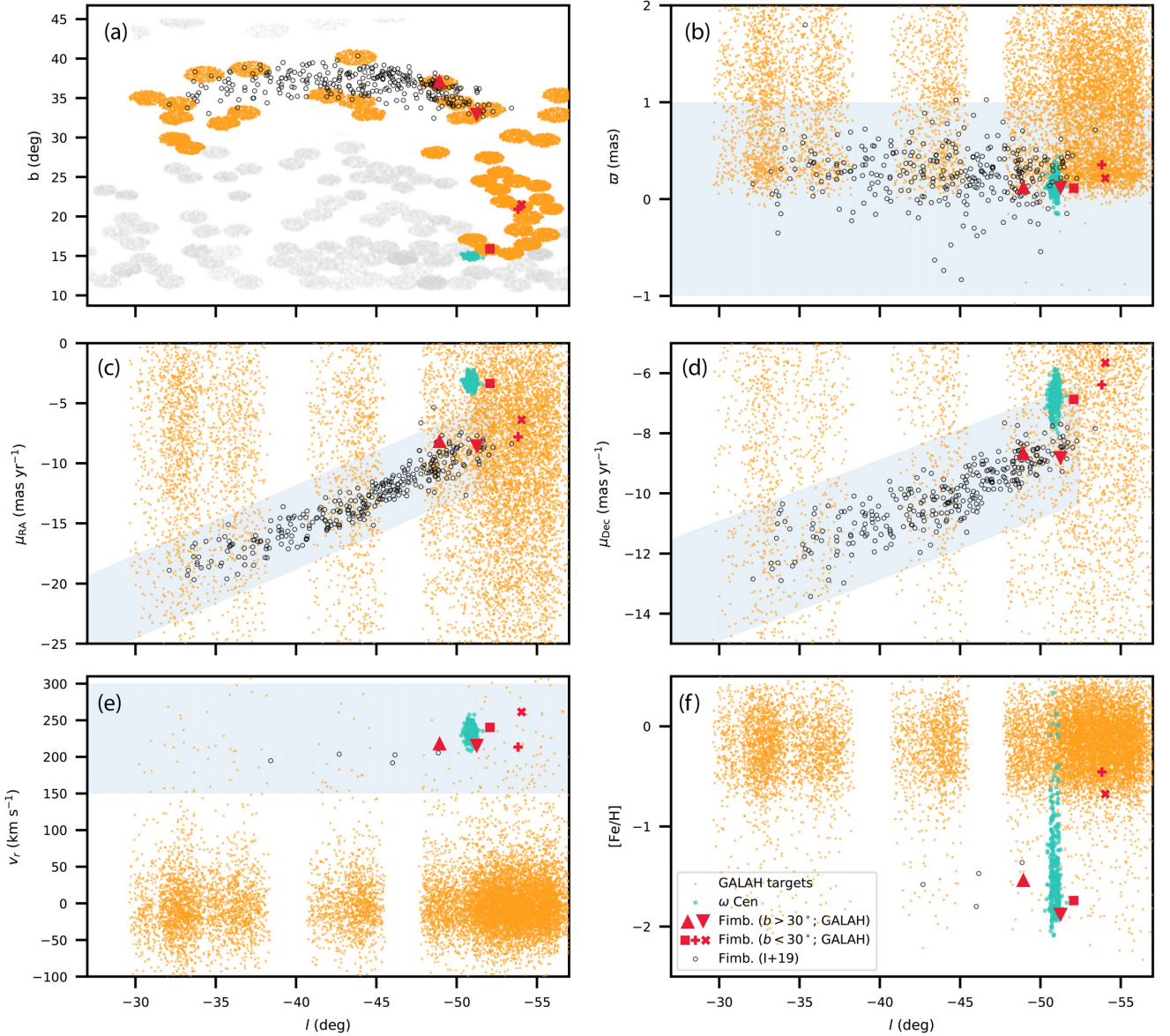
Figure 1. Physical properties of the stars in the region of the sky of ω Cen and the Fimbulthul stream with respect to the Galactic latitude (l). The panels show the: (a) sky distribution of the stars; (b) parallaxes; (c, d) proper motions; (e) radial velocities; and (f) metallicities. In each panel we show the stream members from I + 19 (unfilled black circles), and various groups of stars observed by GALAH: members of ω Cen (turquoise dots), stars along the stream fiducial on the sky (orange dots), candidate stream members (triangle symbols [$b > 30°$], and plus, cross & square symbols [$b < 30°$]). In the first panel we also show the rest of the stars observed by GALAH in this region of the sky as fainter grey dots. The shaded regions in panels (b, c, d, e) graphically show the selection criteria.

by I + 19 for the stream) and parallax in the range $|\varpi| < 1$ mas. For the proper motion criterion, we noted that the proper motion of the stream is approximately linear with Galactic longitude, so a straight line was fitted to this correlation, and it was required that μ_{RA} and μ_{Dec} of stars were within 3.4 and 1.9 mas yr^{-1} respectively of these linear fits (these limits were chosen to encompass almost all of the members identified by I + 19; they are shown as the shaded regions on Figs 1b and c). These criteria identified two stars observed by the GALAH survey that are consistent with the sky position and kinematic properties of the Fimbulthul stream, but had not been associated with the stream by I + 19. Their details (`source_id` of `source_id` of 6...480 and 6...376) are given in Tables 1 and 2 and they are shown as large red triangle symbols in Figs 1, 2, 4, 5, and A1.

For the zone of avoidance region, we selected the stars observed by GALAH that are along the likely fiducial line of the stream (see fig. 1 of I + 19). We used the same radial velocity and parallax criteria as above, but with a proper motion selection of $-10 < \mu_{RA} < -3$ mas yr^{-1}, and $-10.0 < \mu_{Dec} < -5.5$ mas yr^{-1}, again based upon fig. 1 of I + 19. These criteria identified three stars that could possibly be associated with ω Cen and the Fimbulthul stream. Their details are given in Tables 1 and 2 and they are shown as the cross, plus, and square symbols in Figs 1, 2, 4, 5, and A1.

The two stars at the location of the stream (i.e. $b > 30$ deg) are metal poor ([Fe/H] < -1.0), but only one of the zone of avoidance stars (6...064) is very metal poor: [Fe/H] $= -1.74$. The other two stars are only relatively metal poor: [Fe/H] $= -0.46$ and -0.68. We explore the abundance properties of the stars further in Section 4,

Table 1. Observed parameters for the Fimbulthul stream candidate stars as determined by *Gaia* and the GALAH survey.

source_id	Symbol	l (deg)	b (deg)	v_{rad} (km s^{-1})	$G_{BP} - G_{RP}$	G	T_{eff} (K)	log g	[Fe/H]
6192933650707925376	▲	311.06	37.19	218.5	1.03	12.40	5154 ± 130	2.38 ± 0.20	−1.53 ± 0.08
6182748015506372480	▼	308.75	32.86	214.8	1.28	12.17	4509 ± 64	1.24 ± 0.17	−1.88 ± 0.07
6086940734091928064	■	307.93	15.89	240.3	1.34	13.72	4774 ± 248	1.63 ± 0.20	−1.74 ± 0.09
6137654604109711360	✛	306.18	20.92	213.5	1.31	12.83	4806 ± 73	2.16 ± 0.17	−0.46 ± 0.07
6140730767063538048	✖	305.96	21.51	261.4	1.39	13.67	4577 ± 98	2.13 ± 0.20	−0.68 ± 0.08

Table 2. Fimbulthul stream candidate stars observed by the GALAH survey. Elemental abundances with blank entries were those that did not meet the flag_x_fe criteria defined in Section 2. The flag values are given in Table 3. The online version contains all of the ω Cen stars observed by GALAH, and columns for all the elemental abundances.

source_id	Symbol	[Fe/H]	[α/Fe]	[Y/Fe]	[Ba/Fe]	[Na/Fe]	[Al/Fe]
6192933650707925376	▲	−1.53 ± 0.08		0.91 ± 0.09	1.18 ± 0.11	0.29 ± 0.05	0.58 ± 0.05
6182748015506372480	▼	−1.88 ± 0.07	0.18 ± 0.03	− 0.03 ± 0.08	−0.09 ± 0.09	0.23 ± 0.05	0.38 ± 0.04
6086940734091928064	■	−1.74 ± 0.09	0.28 ± 0.04	0.26 ± 0.10	0.77 ± 0.11		
6137654604109711360	✛	−0.46 ± 0.07	0.22 ± 0.02	0.19 ± 0.08	0.28 ± 0.09	0.15 ± 0.05	0.33 ± 0.04
6140730767063538048	✖	−0.68 ± 0.08	0.28 ± 0.03	− 0.06 ± 0.09	−0.20 ± 0.11	0.20 ± 0.06	0.43 ± 0.05

but we note here that although their iron abundance is within the observed distribution of ω Cen (see Fig. 1f), these two more metal-rich stars (6...360, 6...048) do not have the expected s-process abundances for their iron abundance to be chemically tagged to ω Cen (see e.g. Johnson & Pilachowski 2010; Marino et al. 2011b). The very metal-poor star is incidentally the star closest to ω Cen on the sky, less than 1.5 deg from the cluster centre. This places it just outside of the tidal radius of ω Cen ($\sim$1 deg; Da Costa & Coleman 2008).

3.1 Colour-absolute magnitude diagram

Fig. 2 shows the extinction-corrected colour-absolute-magnitude diagram (CMD) of the Fimbulthul stream stars from GALAH and I + 19 stream stars compared to the cluster sequence of ω Cen. The photometry has been adjusted to absolute magnitudes and de-reddened colours, assuming $A_V = 3.1 \times E(B - V)$, and the reddening and extinction corrections are from equation (1) and table 1 of Babusiaux et al. (2018). The $E(B - V)$ values for each star were calculated from the Schlafly & Finkbeiner (2011) reddening maps using the DUSTMAPS interface (Green 2018), except for the ω Cen stars, for which we assumed a single reddening value of $E(B - V) = 0.12$ (Harris 1996).

The distance modulus of ω Cen is well-constrained (e.g. Braga et al. 2018), and we assumed that ω Cen and proposed stream members with $b < 30$ deg are the same distance, namely $(m - M)_0 = 13.7 \equiv 5.5$ kpc. As found in I + 19, the stream and ω Cen are not at the same distance. For the I + 19 sample of Fimbulthul stars, we used a distance modulus of $(m - M)_0 = 12.9 \equiv 3.8$ kpc, i.e. the stream is about 1.7 kpc closer to the Sun than ω Cen. We note that I + 19 had a distance modulus difference between the cluster and the stream of 0.7 mag, compared to our 0.8 mag.

The photometry of the bluest of the GALAH stars on the stream (6...376) places it on the asymptotic giant branch (AGB) of ω Cen. We also inspected CMDs generated from SkyMapper DR2 (Onken et al 2019, in preparation) and Pan-STARRS1 DR2 (Chambers et al. 2016), finding the same result, i.e. 6...376 is clearly bluer than the RGB for its luminosity. This is consistent with the GALAH Kiel diagram (Fig. 2b), which identifies it as an AGB star from its T_{eff} and log g.

4 CHEMICAL TAGGING

As discussed in Section 1, globular clusters, and in particular ω Cen, display star-to-star abundance patterns that are not observed in the vast majority of field stars. Relevant to this work, the elemental abundances of stars in ω Cen have been found to cover large ranges in light elements (e.g. sodium[3] and aluminium). In addition, unlike almost every other globular cluster, the stars also exhibit a large range of iron abundances ($-2.0 <$ [Fe/H] < -0.5) and the abundances of s-process elements (e.g. lanthanum, yttrium, and barium; see e.g. Norris & Da Costa 1995a,b; Johnson & Pilachowski 2010; Stanford, Da Costa & Norris 2010; Marino et al. 2012; Simpson & Cottrell 2013). These provide useful markers for chemically tagging stars to ω Cen.

In Fig. 3 we show small regions of the HERMES spectrum surrounding the regions used by THE CANNON for Na, Ba, and Y abundance determination. Spectra of the two new Fimbulthul stream stars are shown with heavier red lines, and spectra of other GALAH stars with similar stellar parameters but different elemental abundances are shown with thin lines colour-coded by their abundance. The higher Ba and Y abundances in 6...376 and the enhanced Na abundance in both stars can be seen directly in the spectra. In Fig. 4. we show the iron abundance, [α/Fe], and abundance distributions for [Y/Fe], [Ba/Fe], [Na/Fe], and [Al/Fe] for the 40 040 stars in the region of the sky within the box $10° < b < 45°$ and $-27° < l < -57°$ (i.e. the region of the sky shown in Fig. 1a). The abundances of the ω Cen stars and our proposed Fimbulthul stream members observed by GALAH are highlighted. The full abundance set is shown in Fig. A1.

Overall, our results show that we recover the known iron abundance distribution of ω Cen,[4] with most of the stars much

---

[3] Although oxygen is typically part of the analysis of second population stars in globular clusters, the wavelength coverage of HERMES does not include useful oxygen lines in cool, metal-poor giants. It would therefore be useful to follow up these stars (e.g. in the infrared) to obtain oxygen abundances.
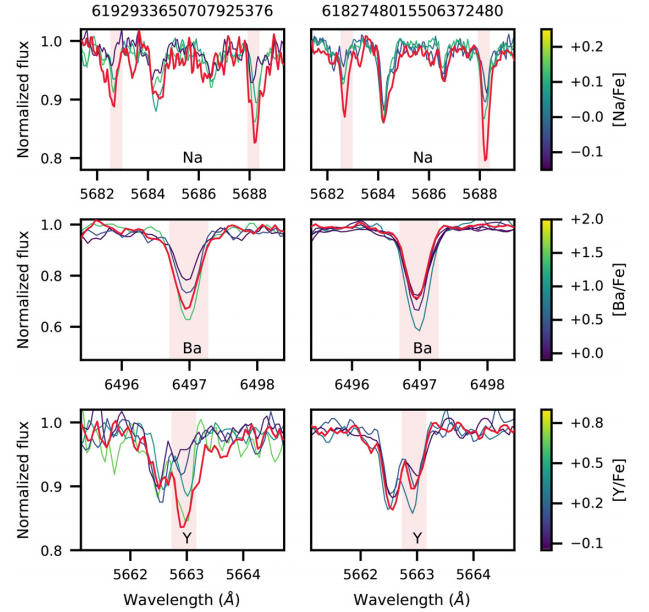[4] Four of the ω Cen stars have implausible, supersolar iron abundances. In the provisional internal third data release of GALAH, these stars have much more reasonable metallicities of [Fe/H] ~ -0.7, while the other ω Cen stars are relatively unchanged.
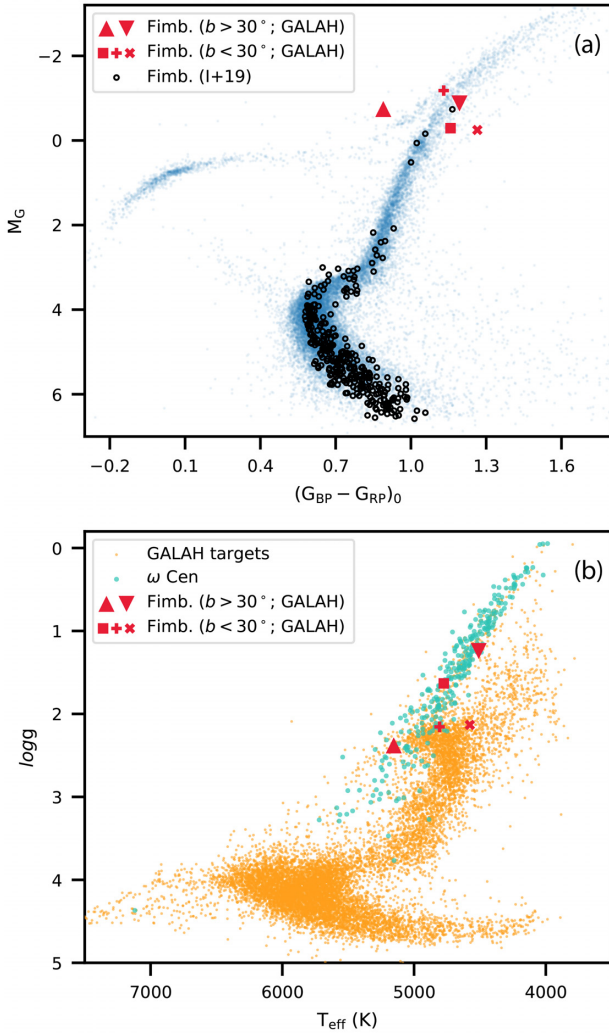
Figure 2. (a) Absolute and dereddened colour-magnitude diagram of ω Cen in *Gaia* DR2 photometry, with the stars selected as described in Section 2. Overplotted are the candidate stream members from GALAH (with the same symbols as Fig. 1; red triangle symbols [b > 30°], and red plus, cross & square symbols [b < 30°]); and the Fimbulthul stars from I + 19 (open black circles). (b) T_{eff}-log g diagram of the region of the sky shown in Fig. 1, highlighting the ω Cen and Fimbumthul stars.


Figure 3. Continuum normalized spectra for 6...376 (left-hand column) and 6...480 (right-hand column) highlighting the bandpasses used for determining the elemental abundances for Na (top row), Ba (middle row), and Y (bottom row) in GALAH DR2. In each panel are the spectra of stars from the GALAH DR2 data set with T_{eff}, log g, and [Fe/H] within ±100 K, ±0.5 dex, ±0.03 dex respectively of our Fimbulthul stream stars, but with a range of abundances in the given element. These spectra are colour coded by their [X/Fe]. These plots show that the two stream stars have stronger Na lines than stars of the same of stellar parameters, while 6...376 has strong Ba and Y lines and 6...480 has weaker lines for these elements.

more metal poor than the bulk of the stars in this region of the sky. For the light elements [Na/Fe] and [Al/Fe], we find the large star-to-star abundance ranges known to exist in ω Cen (e.g. Norris & Da Costa 1995a). The two stars identified in the Fimbulthul region (i.e. b > 30 deg) also are enhanced in these elements, strongly indicative of them being second population globular cluster stars. In Fig. 5(a), we highlight the correlation between [Na/Fe] and [Al/Fe] for all stars with [Fe/H] < −0.8 observed by GALAH in this region of the sky. The bulk of the field stars have [Al/Fe] and [Na/Fe] less than 0.4 dex, but many of the ω Cen stars are enhanced in these elements like the two GALAH-Fimbulthul stars.

Further evidence for chemically tagging these stars to ω Cen can be found in their s-process abundances. The ω Cen stars show the characteristic rapid increase in s-process abundance with iron found in other work. The star that is more metal rich (6...376) has [Y/Fe] = 0.9 and [Ba/Fe] = 1.2. Fig. 5(b) shows that such abundances are rarely seen in the field. Finding a metal-poor star

that is both enhanced in s-process elements and light elements like aluminium is rare. There are ∼20 stars with [Fe/H] < −1.0 in the entire GALAH data set with [Ba/Fe] > 1.0 and [Al/Fe] > 0.4 and most are found in ω Cen. The other stars with enhanced light element abundances warrant follow up to understand their origins. The more metal-poor star (6...480; the reddest GALAH-Fimbulthul star on Fig. 2) shows no enhancement in [Y/Fe] nor [Ba/Fe] relative to the field, but this would be expected at its iron abundance if it had been lost from ω Cen.

Both 6...480 and 6...376 have second population abundances, they follow the [Fe/H]-[s/Fe] trend of ω Cen, and they are spatially and kinematically compatible with being members of the Fimbulthul stream. As a result, we are confident about chemically tagging these stars to ω Cen, and therefore the rest of the Fimbulthul stream to ω Cen.

We now briefly consider the three stars from the zone of avoidance (i.e. b < 30, outside of the region considered by Ibata et al. 2019b). The abundances of two metal-rich stars are not consistent with their being former members of ω Cen. Although somewhat enhanced in light elements, they do not show the level of enhancement in s-process elements expected for an ω Cen star of their iron abundance (see e.g. Johnson & Pilachowski 2010; Marino et al. 2011b). Unfortunately, the extratidal star closest to ω Cen did not have reliable light element abundances, but it does have a moderate enhancement in its s-process abundances. Its closeness to the cluster (only 1.5 deg away), and kinematics basically identical to rest of the cluster point to it being a relatively recently escaped extratidal star. Its position on the sky aligns with the direction of the extratidal features found by I + 19.
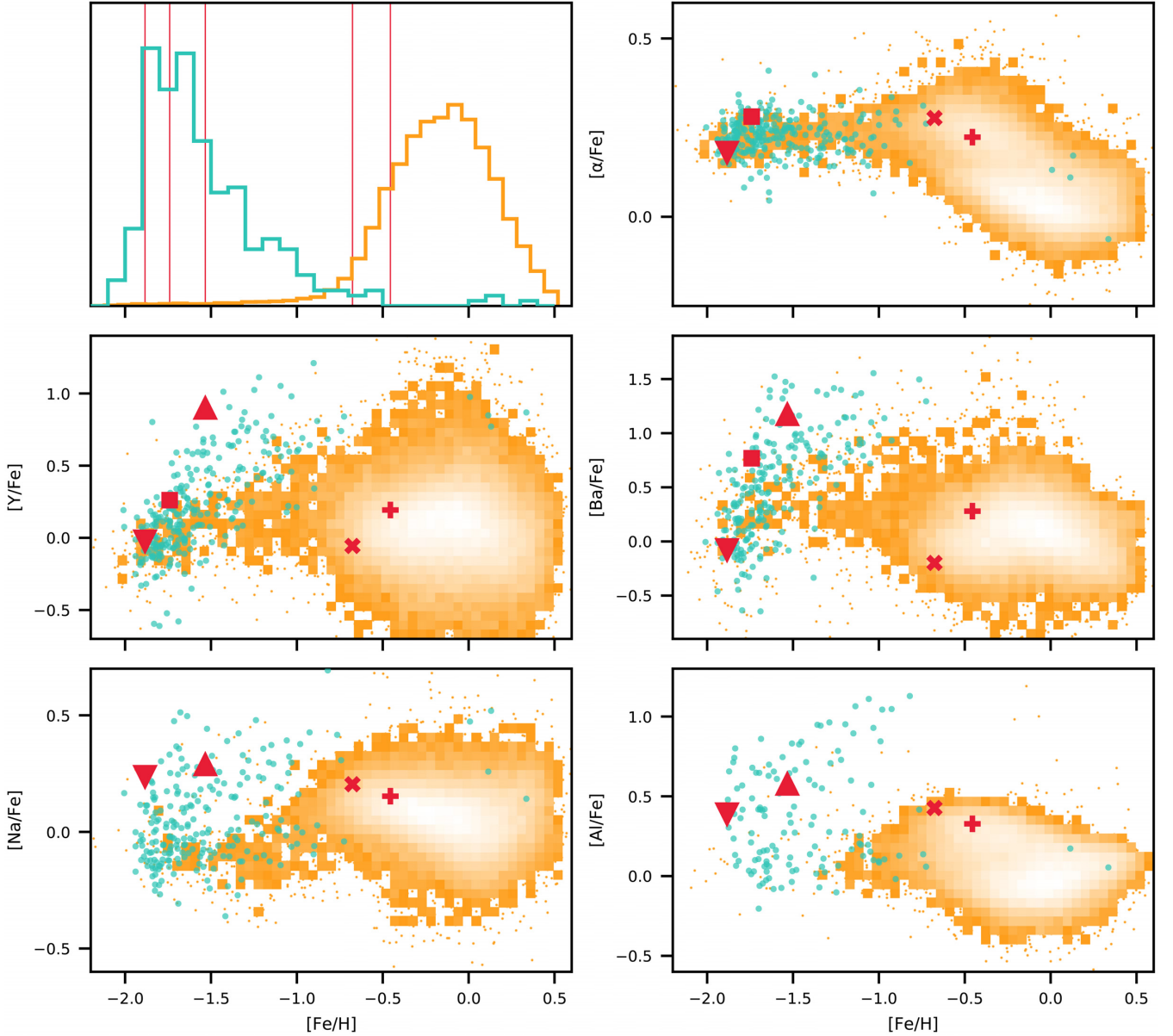
Figure 4. Distributions of (top-left panel) iron abundance, and (remaining panels) [α/Fe], [Y/Fe], [Ba/Fe], [Na/Fe], and [Al/Fe] against [Fe/H] as determined by the GALAH survey for stars in the region of the sky around ω Cen and the candidate Fimbulthul stream members identified in this work. The top-left panel shows the normalized iron abundance distributions of the cluster (turquoise distribution) and field (orange distribution). The vertical red lines mark the iron abundances of our candidate stream members. In the remaining panels is a log-scaled colour density map, with the lightest squares containing the most stars (truncated at three stars per bin; below that threshold, individual stars are plotted as orange dots). The distributions for ω Cen (turquoise dots) and the candidate Fimbulthul stream stars observed by GALAH (same symbols as in Fig. 1; red triangle symbols [$b > 30°$], and red plus, cross and square symbols [$b < 30°$]) are overlaid. For [α/Fe], we find a distribution of ω Cen like that of other metal-poor stars. For [Na/Fe] and [Al/Fe] we find the characteristic star-to-star abundance dispersions previously observed in ω Cen, and that the two GALAH-Fimbulthul stars (red triangle symbols) are enhanced in these elements. In the s-process elements we find the well-known correlation between iron abundance and s-process elemental abundance, with one of the GALAH-Fimbulthul stars very enhanced in yttrium and barium. For the stars from the zone of avoidance region, it is likely that the two metal-rich stars (red plus and cross) are not related to ω Cen due in particular to their s-process abundances.

4.1 Abundance flagging

As discussed in Section 2, we have included stars in our sample that were flagged as having potentially unreliable abundance values. In Table 3 we give the `flag_cannon` and `flag_x_fe` values for the five stars highlighted throughout this work. Of note is that the two likely Fimbulthul stream stars (6...480 and 6...376) both have their [Ba/Fe], [Na/Fe], and [Al/Fe] abundances flagged as either 1 (THE CANNON started to extrapolate) or 2 (Line strength below 2-σ upper

limit). In the case of the `flag_x_fe = 1`, this occurs because the training set does not include metal-poor stars with abundances like those seen in second population globular cluster stars. As such, THE CANNON needs to extrapolate in order to estimate abundances. This does not necessarily mean that the values are inaccurate; moreover abundance accuracy is not the key aim of this work. Instead, our goal was to identify stars with enhanced abundances of light elements relative to the bulk of the metal-poor halo population, in order to
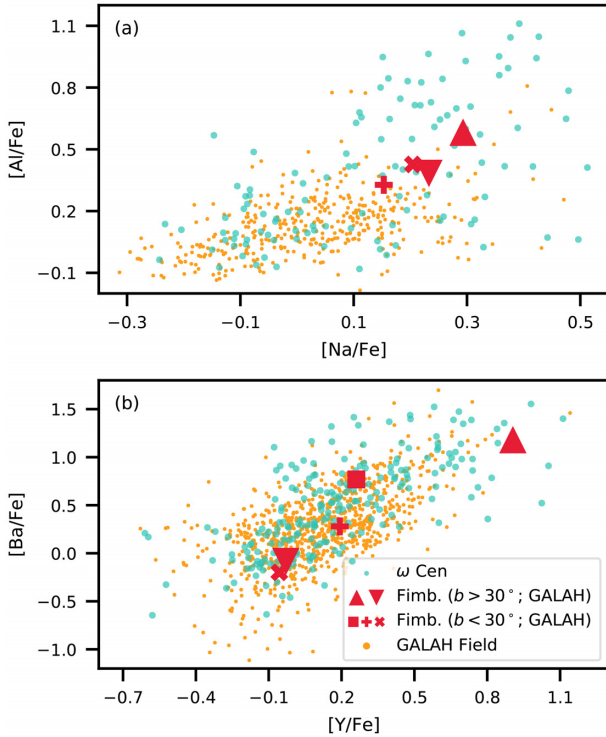
Figure 5. Abundance distributions of ω Cen compared to all other metal-poor stars ([Fe/H] < −0.8) observed by GALAH in the region of the sky shown in Fig. 1. (a) [Na/Fe] against [Al/Fe] (i.e. light elements); and (b) [Y/Fe] against [Ba/Fe] (i.e. s-process elements). About half of the ω Cen stars (turquoise dots) and the two candidate Fimbulthul stars with b > 30 deg (red triangles) have enhanced light elements compared to the bulk of the other metal-poor stars. Most of the field stars have [Al/Fe] ∼ 0, while the ω Cen stars extend up to [Al/Fe] ∼ 1. For the s-process elements, there is a large range in the field, but the one candidate Fimbulthul star is even more enhanced in [Y/Fe] than the majority of field stars.

chemically tag them as second population ω Cen stars. We can be confident that THE CANNON will have estimated abundances that reflect these stars are enhanced in the particular elements of interest.

4.2 Abundances on the asymptotic giant branch

As noted in Section 3, 6...376 is an AGB star. There has been much discussion in the literature about differences in the abundances of stars on the AGB versus those on the RGB in globular clusters (Norris et al. 1981; Campbell et al. 2013, 2017; MacLean et al. 2016, 2018), in particular with respect to apparent differences in their derived metallicities and light element abundances (Lapenna et al. 2016; Mucciarelli et al. 2019). There are two related effects that

are causing these discrepancies. First, the iron abundance derived from neutral and ionized species differ in AGB stars. Secondly, on the AGB, the T_{eff} derived from the infrared flux method gives significantly different values to those derived from spectroscopic analysis – while in RGB stars, the two methods give the same values. These discrepancies are likely the result of the current treatment of stellar atmospheres using 1D-LTE, and the potential for 3D and/or NLTE effects to be larger in AGB stars than in RGB stars. For GALAH DR2 abundances there was an effort to include non-LTE calculations for key elements, including Na and Al (Buder et al. 2018).

5 CONCLUDING REMARKS

In this work, we have shown that two stars observed by the GALAH survey are associated with the Fimbulthul stellar stream and can be chemically tagged to the massive globular cluster ω Cen. We find another star that has likely just escaped from the cluster. ω Cen is the most massive of the Milky Way's ∼160 known clusters and has a broad iron distribution, abundance patterns not otherwise seen in globular clusters, and a retrograde orbit about the Galaxy. This has led to the hypothesis that ω Cen is the core of an accreted dwarf galaxy. The progenitor galaxy of ω Cen would have been 10^3 to 10^4 times larger than the present day mass of ω Cen (Tsuchiya, Dinescu & Korchagin 2003; Tsuchiya, Korchagin & Dinescu 2004), which means that there should be tidal tails and debris lost from ω Cen and its host galaxy throughout the Milky Way. Confirming the association of Fimbulthul to ω Cen by I + 19 marks the first time that tidal arms have been found well away from the cluster.

Overall, we have only identified three stars observed by GALAH, outside of the tidal radius that we are confident to associate with ω Cen. As discussed in Da Costa & Coleman (2008), the current orbit of ω Cen is such that it is strongly influenced by tidal shocks. Stars leaving the cluster with a relative velocity of ∼1 km s^{-1} (the velocity dispersion in the outer parts is a few km s^{-1}; see, e.g. Da Costa 2012) can transverse the region between 1 and 2 tidal radii in less than the orbital period around the Galaxy. At this point the next disc crossing likely gives them sufficient kick to move further away. As such, we would expect there to be few stars remaining close to cluster – there is effectively just too much gravitational energy being pumped in. Note that this is quite different to the situation for an orbit with a larger ratio of Galactic apocentre to pericentre, in which the unbound stars do not dissipate as rapidly and we would expect tidal debris near the cluster.

In the next few years, both the *Gaia* and GALAH surveys should produce their third data releases, which will add a vast amount of new and improved data by which our study could be expanded. Having demonstrated here the power of chemical tagging in aiding

Table 3. Stellar parameter and elemental abundance flagging for the five stars of interest from the GALAH survey. Values of zero indicate there are known reliability problems with the value. +1 flags that THE CANNON had started to extrapolote; +2 flags that the line strength was below the 2-σ upper limit. For 6086940734091928064, the values for [Na/Fe] and [Al/Fe] (e.g. ≥4) show that this elemental abundance had multiple reliability problems.

source_id	sobject_id	Symbol	flag_cannon	flag_y_fe	flag_ba_fe	flag_na_fe	flag_al_fe
6192933650707925376	170512001301266	▲	0	1	1	1	2
6182748015506372480	170513003501228	▼	0	0	2	1	1
6086940734091928064	170404002101197	■	0	0	0	4	5
6137654604109711360	170408004001066	✚	0	0	0	0	0
6140730767063538048	170408004001278	✖	0	0	0	0	0

the identification of stellar streams from ω Cen, it will be interesting to see whether those new and expanded data sets allow us to further strengthen the connection between the Fimbulthul stream and ω Cen, and to potentially draw conclusions on the time-scales on which the disruption of the postulated progenitor galaxy by the Milky Way has occurred.

REFERENCES

Babusiaux C. et al., 2018, A&A, 616, A10
Bastian N., Lardo C., 2018, ARA&A, 56, 83
Bekki K., Freeman K. C., 2003, MNRAS, 346, L11
Bellazzini M., Ibata R. A., Martin N., Malhan K., Marasco A., Famaey B., 2019, MNRAS, 490, 2588
Belokurov V., Evans N. W., Irwin M. J., Hewett P. C., Wilkinson M. I., 2006, ApJ, 637, L29
Bland-Hawthorn J., Krumholz M. R., Freeman K., 2010, ApJ, 713, 166
Bonaca A., Hogg D. W., Price-Whelan A. M., Conroy C., 2019, ApJ, 880, 38
Braga V. F. et al., 2018, AJ, 155, 137
Brown A. G. A. et al., 2018, A&A, 616, A1
Buder S. et al., 2018, MNRAS, 478, 4513
Campbell S. W. et al., 2013, Nature, 498, 198
Campbell S. W., MacLean B. T., D'Orazi V., Casagrande L., de Silva G. M., Yong D., Cottrell P. L., Lattanzio J. C., 2017, A&A, 605, A98
Carballo-Bello J. A., 2019, MNRAS, 486, 1667
Caswell T. A. et al., 2019, matplotlib/matplotlib v3.1.0. Available at: https://doi.org/10.5281/zenodo.2893252
Chambers K. C. et al., 2016, preprint (arXiv:1612.05560)
Cole S., Lacey C. G., Baugh C. M., Frenk C. S., 2002, MNRAS, 319, 168
Côté P., Marzke R. O., West M. J., 1998, ApJ, 501, 554
Côté P., Marzke R. O., West M. J., Minniti D., 2000, ApJ, 533, 869
Da Costa G. S., 2012, ApJ, 751, 6
Da Costa G. S., Coleman M. G., 2008, AJ, 136, 506
De Silva G. M. et al., 2015, MNRAS, 449, 2604
Dotter A., Milone A. P., Conroy C., Marino A. F., Sarajedini A., 2018, ApJ, 865, L10
Evans D. W. et al., 2018, A&A, 616, A4
Eyre A., Binney J., 2009, MNRAS, 400, 548
Fernández-Trincado J. G. et al., 2015, A&A, 583, A76
Fernández-Trincado J. G. et al., 2016, ApJ, 833, 132
Fernández-Trincado J. G. et al., 2017, ApJ, 846, L2
Freeman K., Bland-Hawthorn J., 2002, ARA&A, 40, 487
Green G. M., 2018, J. Open Source Softw., 3, 695
Harris W. E., 1996, AJ, 112, 1487
Hasselquist S. et al., 2019, ApJ, 872, 58
Helmi A. et al., 2018, A&A, 616, A12
Hunter J. D., 2007, Comput. Sci. Eng., 9, 90
Ibata R. A., Malhan K., Martin N. F., Starkenburg E., 2018, ApJ, 865, 85
Ibata R. A., Bellazzini M., Malhan K., Martin N., Bianchini P., 2019a, Nat. Astron., 3, 667
Ibata R. A., Malhan K., Martin N. F., 2019b, ApJ, 872, 152
Johnson C. I., Pilachowski C. A., 2010, ApJ, 722, 1373
Koppelman H., Helmi A., Veljanoski J., 2018, ApJ, 860, L11
Kos J. et al., 2016, MNRAS, 464, 1259
Kos J. et al., 2017, MNRAS, 473, 4612
Kos J. et al., 2018, MNRAS, 480, 5242
Kuzma P. B., Da Costa G. S., Mackey A. D., 2018, MNRAS, 473, 2881
Lapenna E. et al., 2016, ApJ, 826, L1
Law D. R., Majewski S. R., 2010, ApJ, 714, 229
Lewis I. J. et al., 2002, MNRAS, 333, 279
Lind K. et al., 2015, A&A, 575, L12
Lindegren L., 2018, Technical Report, Re-normalising the Astrometric Chi-Square in Gaia DR2. Lund Observatory. Available at: http://www.rssd.esa.int/doc_fetch.php?id = 3757412
Li T. S. et al., 2019, MNRAS, 490, 3508
Lynden-Bell D., Lynden-Bell R. M., 1995, MNRAS, 275, 429
MacLean B. T., Campbell S. W., De Silva G. M., Lattanzio J., D'Orazi V., Simpson J. D., Momany Y., 2016, MNRAS, 460, L69
MacLean B. T. et al., 2018, MNRAS, 481, 373
Malhan K., Ibata R. A., 2018, MNRAS, 477, 4063
Malhan K., Ibata R. A., 2019, MNRAS, 486, 2995
Malhan K., Ibata R. A., Martin N. F., 2018, MNRAS, 481, 3442
Marconi M. et al., 2014, MNRAS, 444, 3809
Marino A. F. et al., 2011a, A&A, 532, A8
Marino A. F. et al., 2011b, ApJ, 731, 64
Marino A. F. et al., 2012, ApJ, 746, 14
Martell S. L., Grebel E. K., 2010, A&A, 519, A14
Martell S. L., Smolinski J. P., Beers T. C., Grebel E. K., 2011, A&A, 534, A136
Martell S. L. et al., 2017, MNRAS, 465, 3203
Mateu C., Read J. I., Kawata D., 2018, MNRAS, 474, 4112
McKinney W., 2010, in van der Walt S., Millman J., eds, 9th Python Sci. Conf.. SciPy, Austin, USA, p. 51
Meingast S., Alves J., Fürnkranz V., 2019, A&A, 622, L13
Miszalski B., Shortridge K., Saunders W., Parker Q. A., Croom S. M., 2006, MNRAS, 371, 1537
Mucciarelli A., Lapenna E., Lardo C., Bonifacio P., Ferraro F. R., Lanzoni B., 2019, ApJ, 870, 124
Myeong G. C., Evans N. W., Belokurov V., Sanders J. L., Koposov S. E., 2018, MNRAS, 478, 5449

Ness M., Hogg D. W., Rix H.-W., Ho A. Y. Q., Zasowski G., 2015, ApJ, 808, 16

Nidever D. L. et al., 2019, preprint (arXiv:1910.05360)

Norris J., Cottrell P. L., Freeman K. C., Da Costa G. S., 1981, ApJ, 244, 205

Norris J. E., Da Costa G. S., 1995a, ApJ, 441, L81

Norris J. E., Da Costa G. S., 1995b, ApJ, 447, 680

Odenkirchen M. et al., 2001, ApJ, 548, L165

Olszewski E. W., Saha A., Knezek P., Subramaniam A., de Boer T., Seitzer P., 2009, AJ, 138, 1570

Oser L., Ostriker J. P., Naab T., Johansson P. H., Burkert A., 2010, ApJ, 725, 2312

Palau C. G., Miralda-Escudé J., 2019, MNRAS, 488, 1535

Piskunov N., Valenti J. A., 2016, A&A, 597, A16

Price-Whelan A. M., Nidever D. L., Choi Y., Schlafly E. F., Morton T., Koposov S. E., Belokurov V., 2018a, preprint (arXiv:1811.05991)

Price-Whelan A. M. et al., 2018b, AJ, 156, 123

Prusti T. et al., 2016, A&A, 595, A1

Quillen A. C. et al., 2018, MNRAS, 478, 228

Robitaille T. P. et al., 2013, A&A, 558, A33

Schiavon R. P. et al., 2017, MNRAS, 465, 501

Schlafly E. F., Finkbeiner D. P., 2011, ApJ, 737, 103

Searle L., Zinn R., 1978, ApJ, 225, 357

Sheinis A. et al., 2015, J. Astron. Telesc. Instrum. Syst., 1, 35002

Simpson J. D., Cottrell P. L., 2013, MNRAS, 433, 1892

Simpson J. D., Cottrell P. L., Worley C. C., 2012, MNRAS, 427, 1153

Simpson J. D. et al., 2019, MNRAS, 482, 5302

Skrutskie M. F. et al., 2006, AJ, 131, 1163

Stanford L. M., Da Costa G. S., Norris J. E., 2010, ApJ, 714, 1001

Tang B., Liu C., Fernández-Trincado J. G., Geisler D., Shi J., Zamora O., Worthey G., Moreno E., 2019, ApJ, 871, 58

Taylor M. B., 2005, in Shopbell P., Britton M., Ebert R., eds, ASP Conf. Ser. Vol. 347, ADASS XIV. Astron. Soc. Pac., San Francisco, p. 29

Tody D., 1986, in Crawford D. L., ed., Proc. SPIE Conf. Ser. Vol. 0627, The Iraf Data Reduction And Analysis System. SPIE, Bellingham, p. 733

Tsuchiya T., Dinescu D. I., Korchagin V. I., 2003, ApJ, 589, L29

Tsuchiya T., Korchagin V. I., Dinescu D. I., 2004, MNRAS, 350, 1141

Valenti J. A., Piskunov N., 1996, A&AS, 118, 595

Venn K. A., Irwin M., Shetrone M. D., Tout C. A., Hill V., Tolstoy E., 2004, AJ, 128, 1177

Villanova S., Geisler D., Carraro G., Moni Bidin C., Muñoz C., 2013, ApJ, 778, 186

White S. D. M., Frenk C. S., 1991, ApJ, 379, 52

SUPPORTING INFORMATION

Supplementary data are available at *MNRAS* online.

Table 1. Observed parameters for the Fimbulthul stream candidate stars as determined by *Gaia* and the GALAH survey.
Table 2. Fimbulthul stream candidate stars observed by the GALAH survey.

Please note: Oxford University Press is not responsible for the content or functionality of any supporting materials supplied by the authors. Any queries (other than missing material) should be directed to the corresponding author for the article.

APPENDIX A: FULL ABUNDANCE SET
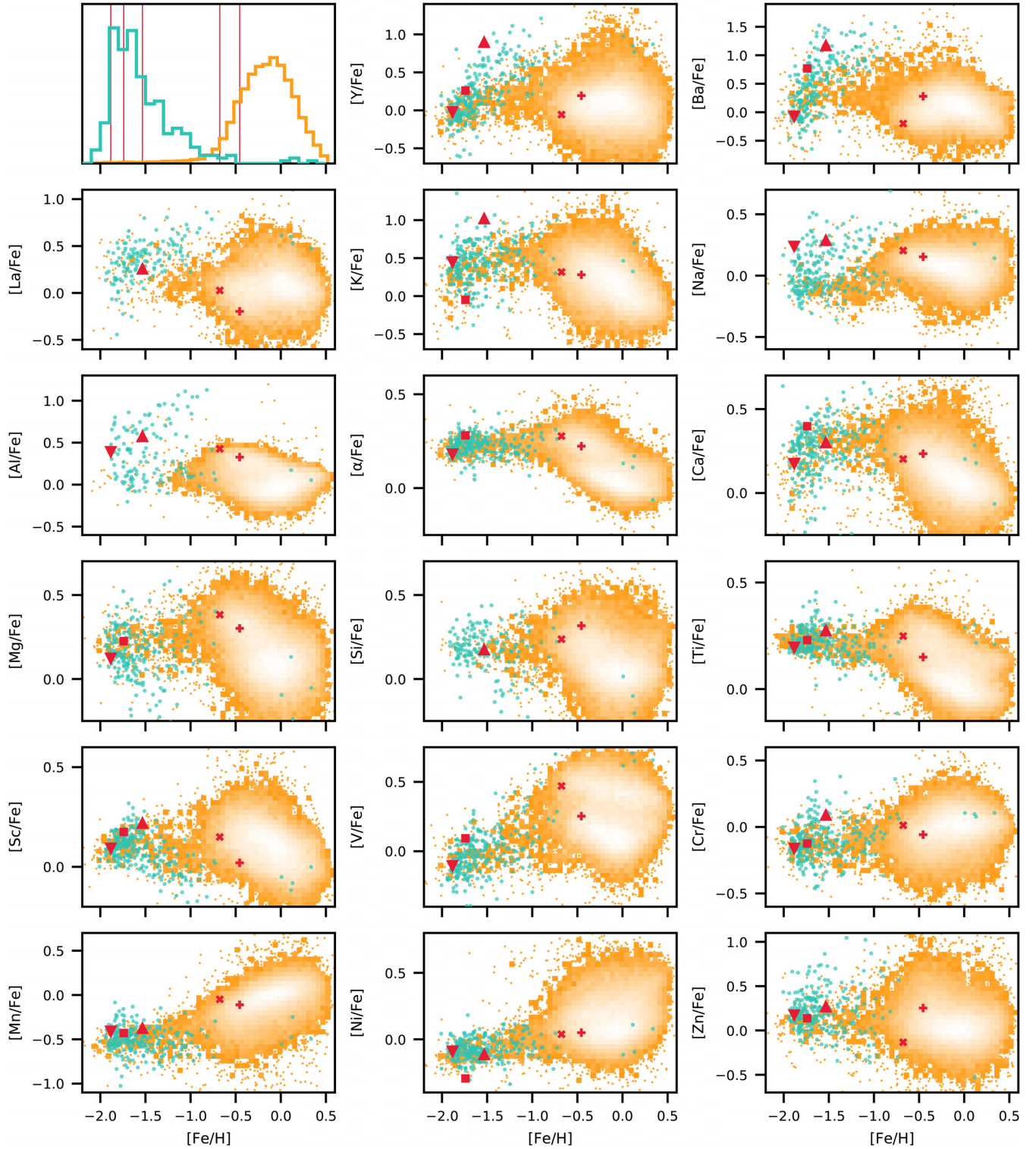
Figure A1. The same as Fig. 4 but for the entire set of elemental abundances available within the GALAH catalogue.